Engineering Transactions, **72**(4): 403–422, 2024, doi: 10.24423/EngTrans.3316.2024
Institute of Fundamental Technological Research Polish Academy of Sciences (IPPT PAN)
Université de Lorraine • Poznan University of Technology

Research Paper

Design of a Non-Circular Gear-Crank Slider Baler Mechanism Considering Slider Acceleration

Jian WANG*, Chenjie WANG, Long MIAO

School of Mechanical Engineering, Nanjing Institute of Technology
Nanjing Jiangsu, 211167, China

*Corresponding Author e-mail: xmwjian@163.com

A design method considering slider acceleration is proposed to reduce vibration and improve the working efficiency of a non-circular gear-crank slider baler mechanism. The ideal kinematic curves such as the displacement, velocity and acceleration curves of this proposed non-circular gear-crank slider hay baler mechanism are established. The slider strokes are divided into the working stroke and return stroke. The pitch curve of the non-circular gear is established during the slider's working stroke based on curve smoothness characteristics and the pitch curve sealing condition. Using a compensation method, the corresponding pitch curve is constructed for the slider's return stroke. Additionally, the design process of non-circular gear-crank slider hay baler mechanism is described in detail with special consideration given to slider acceleration. An assembly model of the non-circular gear-crank slider hay baler mechanism is created with the involute as the tooth profile. Consequently, a movement simulation is carried out using ADAMS software, and the obtained kinematic curves matched the curves established initially. The research results indicate that the proposed baler mechanism exhibits lower speed fluctuation. Additionally, the maximum power and maximum acceleration required by the proposed baler mechanism are reduced by 66.4% and by an order of magnitude, respectively, compared to an existing non-circular gear-crank slider hay baler mechanism.

Keywords: agricultural machinery; baler mechanism; non-circular gear; crank slider; acceleration.

1. Introduction

There is an abundance of natural forage crops, especially in China. However, if these forages crops are not packed properly, they will require more space, which can drive up storage and transportation costs [1]. A common solution is to use a baler to compact the crops. According to existing literature, the density of baled hay can increase by ten times compared to non-baled hay, and the transportation cost can be potentially reduced by around 70% [2].

The most common slider-crank mechanism balers in the commercial industry are John Deer 349 and Mercedes-Benz 88A. These balers use a slider-crank mechanism, known for being simple, reliable and having a low failure-rate. However, this type of mechanism has limitations: compression speed has limitations when resistance is low, and it is slow when resistance increases. Furthermore, the compression time is longer than the return time [3–6]. Many studies have considered ways to improve the movement characteristics of the slider/crank mechanism by optimizing the structure through and using virtual simulations. Wang and Tan [7] used a virtual prototype to simulate and analyze the baling process of forage. An ADAMS model of the compression process was established in the form of spring-damper parallel connection, and model's structure and method were verified. Zhao [8] established a dynamic equation for the baler's compression mechanism and conducted a dynamic analysis of the compression mechanism. Li *et al.* [9] designed a six-bar baler mechanism and carried out kinematics and dynamics simulations. The results showed that the six-bar baler mechanism requires less manual labor compared to the traditional crank-slider mechanism. Chen *et al.* [10] proposed a cam-type baler mechanism. The simulation results demonstrated fast pre-compression stage and slower compression stages. While the existing literature presents several methods to improve working efficiency and reduce energy consumption, to the authors' best knowledge, none of the current baling mechanisms has been optimized based on movement characteristics.

The shape and movement characteristics of a non-circular gear are determined by its pitch curves [11–13]. The pitch curves of a non-circular gear consist of multi-segment curves, which can be used to adjust rotational speed, change rotational direction, or adjust cycle time. These features allow the mechanism to achieve constant-speed movement during the working stroke, the rapid return movement of empty return stroke, and to increase or decrease the stroke's speed [14–18]. Lei *et al.* [4] applied this type of non-circular gear to a baler mechanism and carried out parameter inversion. The results showed that the compression time in a working cycle for the non-circular gear-crank slider hay baler mechanism increased by 30%, while the required maximum input power was reduced by 28.6% compared to traditional slider-crank baler mechanisms. The ideal velocity curve of the slider was used to determine the pitch curve and the baler mechanism's geometry. Although this baler mechanism can achieve fast compression in a low-resistance stage and maintain constant low-speed compression in high-resistance stage, only the slider's velocity has been examined. The slider's acceleration has not been examined. It is well known that in a non-circular gear-crank slider mechanism, higher acceleration will increase the inertia forces generated by the slider's high-speed movement in the operational range. These high inertia forces lead to vibration. On the other hand, lower acceleration and speed in the non-operational range will increase the return time and reduce ef-

ficiency [15, 16]. In contrast to the balers currently on the market, one of the main issues in the field of agricultural baler machinery is reducing noise and vibration during the baling process [19, 20].

This paper proposes an inverse design method for a non-circular gear-crank slider baler mechanism, which considers both slider velocity and acceleration. By specifying the desired velocity and acceleration curves for the slider, the pitch curve of the non-circular gear can be inversely calculated using numerical calculation methods and non-circular gear meshing theory. The pitch curve can be effectively controlled by adjusting the slider's velocity and acceleration, leading to the development of a corresponding mathematical model for the non-circular gear-crank slider baler mechanism. Therefore, to reduce vibration and noise during the baling process, the kinematic simulation and baling characteristics of this mechanism are investigated to provide a theoretical basis and technical support for improving operational quality and efficiency.

2. Construction of ideal kinematic curve of the baler mechanism

2.1. Baling principle

According to the compression chamber's structural characteristics, balers can be categorized into two types: closed compression and open compression. In closed compression, the bale chamber is a closed container with a plunger. The compression process of the closed compression starts when forage is fed into the bale's chamber, and the plunger moves to compact the forage. Once compression is complete, the baled forage is removed from the chamber. Figure 1 shows a schematic drawing of the closed compression process.

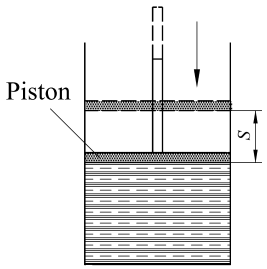

Fig. 1. Schematic diagram of a closed compression baling process.

Open compression takes place in a container without enclosure. The container is mounted on a vehicle chassis, and moves along with it. The bale chamber is mainly composed of a crank, piston (slider), feeding entrance, and exit, as shown in Fig. 2 [21]. The crank is powered by a prime mover, causing the piston

to move in a reciprocating linear motion. Uncompressed forage is fed through the feeding entrance, typically located at the top, and the piston moves to compact it. The forage is then being pushed forward a stroke distance in the bale chamber. As more forage is fed into the bale chamber, the compressed forage exits through the bale's chamber exit, and the process repeats. Open compression is a continuous process, which is more suitable for large-scale baling operations compared to closed compression.

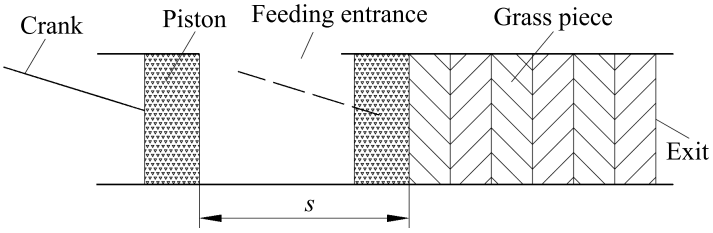

FIG. 2. Schematic diagram of an open compression baling process.

In open compression, the resistance during the baling process is mainly caused by the friction force between the inner container wall and the forage, resulting in varying pressure on the material during the compression process [17]. Considering only the force in the stroke movement's direction, the slider's ideal velocity curve has been established in existing literature [4]. In an ideal baling cycle, the slider runs at a high speed during the low-resistance stage and compresses at a lower speed during the high-resistance stage, and then returns to the starting position at a fast speed.

2.2. Construction of the ideal kinematic curve of the slider with consideration on the slider acceleration

2.2.1. Non-circular gear-crank slider mechanism and transmission ratio. The schematic diagram of a non-circular gear-crank slider mechanism is shown in Fig. 3. The pitch curve diameters of the driving and driven non-circular gears are denoted as r_1 and r_2, respectively. The angular velocities of the non-circular driving and driven non-circular gears are ω_1 and ω_2, respectively. The angles of rotation for the non-circular driving and driven non-circular gears are φ_1 and φ_2, respectively. Parameters l_2 and l_3 are the lengths of the crank O_2A and connecting rod AC, respectively. The center distance is denoted as a, and the slider displacement s can be expressed as a function of the rotation angle φ_1.

It can be seen from Fig. 3 that the rotation angle φ_2 can be expressed as:

$$\varphi_2 = \pi - \arccos \frac{l_2^2 + s^2 - l_3^2}{2 l_2 s}. \tag{2.1}$$

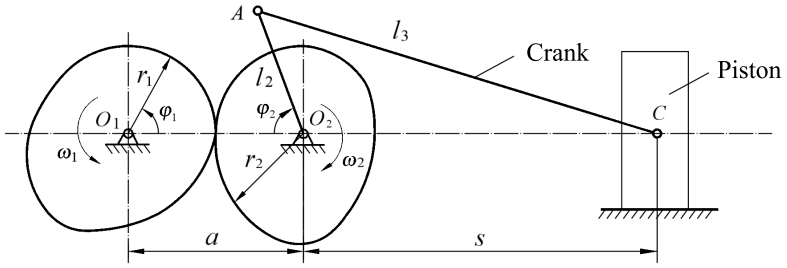

FIG. 3. Schematic diagram of non-circular gear crank slider mechanism.

Let i_{12} be the transmission ratio of the two gears, that is, the ratio of the instantaneous angular velocity of the driving non-circular gear to that of the driven non-circular gear. Then, i_{12} can be expressed as:

$$i_{12} = \frac{\mathrm{d}\varphi_1}{\mathrm{d}\varphi_2}. \tag{2.2}$$

By combining Eq. (2.1) and Eq. (2.2), the transmission ratio of the two gears can be rewritten as:

$$i_{12} = \frac{s\sqrt{4l_2^2 s^2 - \left(l_2^2 + s^2 - l_3^2\right)^2}}{\left(s^2 - l_2^2 + l_3^2\right) v}, \tag{2.3}$$

where v represents the slider movement speed.

2.2.2. Construction of the ideal kinematic curve. To reduce vibration and noise during the baling process, there should be a smooth transition between the slow and fast speeds of the slider. Therefore, it is essential to control both the slider's velocity and acceleration. The ideal displacement and velocity curves of the slider, as established in existing literature [4], are shown in Fig. 4. The

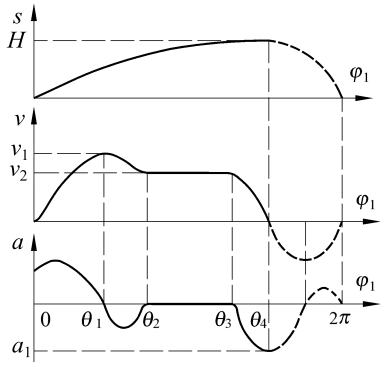

FIG. 4. The ideal displacement, velocity and acceleration curves of the slider.

baler's compression process is divided into the working period (solid line) and the return period (dashed line). According to the slider resistance change curve presented in [4], the ideal velocity curves must satisfy the following conditions: the slider should approach the compression point at a faster rate, then decrease to a suitable speed, compress at a constant rate, and promptly return to its initial position after completing the compression. Based on the continuity condition of the curves and the relationships between velocity and acceleration, the ideal acceleration curve is also given in Fig. 4. The displacement, velocity, and acceleration curves of the slider are designated as s, v, and a, respectively. Among these, the maximum velocity during the working period is v_1, the velocity during the constant movement period is v_2, the acceleration at the beginning of the return period is a_1, and the maximum slider displacement is H.

In this section, a polynomial function is used to describe the ideal movement curve equations for the working period. The return period's kinematic curve is solved by using the constraints of the pitch curve, which will be introduced in the following section. For simplicity, the working strike is divided into three segments: the first motion segment (0–θ_2), the second motion segment (θ_2–θ_3), and the third motion segment (θ_3–θ_4), according to the velocity curve. During these three segments, the slider undergoes acceleration followed by deceleration in the first motion segment, uniform motion in the second motion segment, and deceleration again in the third motion segment. The superscripts b, c, and d are used to represent the parameters of the first, second and third motion segments, respectively. The first motion segment (0–θ_2), The displacement, velocity, and acceleration for the first motion segment (0–θ_2), can be expressed by the following polynomials:

$$s_b = b_0\varphi_1^5 + b_1\varphi_1^4 + b_2\varphi_1^3 + b_3\varphi_1^2 + b_4\varphi_1 + b_5, \tag{2.4}$$

$$v_b = 5b_0\varphi_1^4 + 4b_1\varphi_1^3 + 3b_2\varphi_1^2 + 2b_3\varphi_1 + b_4, \tag{2.5}$$

$$a_b = 20b_0\varphi_1^3 + 12b_1\varphi_1^2 + 6b_2\varphi_1 + 2b_3. \tag{2.6}$$

Among them, the coefficients b_0, b_1, b_2, b_3, b_4, and b_5 are the polynomial coefficients.

Similarly, for the second motion segment (θ_2–θ_3), the displacement, velocity, and acceleration can be expressed as:

$$s_c = c_0\varphi_1 + c_1, \tag{2.7}$$

$$v_c = c_0, \tag{2.8}$$

$$a_c = 0, \tag{2.9}$$

where the coefficients c_0 and c_1 are polynomial coefficients.

For the third motion segment (θ_3–θ_4), the displacement, velocity, and acceleration can be expressed by the following polynomials:

$$s_d = d_0\varphi_1^4 + d_1\varphi_1^3 + d_2\varphi_1^2 + d_3\varphi_1 + d_4, \tag{2.10}$$

$$v_d = 4d_0\varphi_1^3 + 3d_1\varphi_1^2 + 2d_2\varphi_1 + d_3, \tag{2.11}$$

$$a_d = 12d_0\varphi_1^2 + 6d_1\varphi_1 + 2d_2, \tag{2.12}$$

where the coefficients d_0, d_1, d_2, d_3, d_4 are polynomial coefficients.

3. Design of non-circular gear-crank slider mechanism considering slider acceleration

The non-circular gear is crucial for designing a non-circular gear-crank slider mechanism. One of the primary challenges for designing a non-circular gear design is establishing its pitch curve mathematical model. In this section, the mathematical models of the pitch curves for non-circular gears in the working and return periods are established. The pitch curve equation of the driving gear has been established in [22] and can be expressed as:

$$r_1(\varphi_1) = \frac{a}{1 + i_{12}}. \tag{3.1}$$

Additionally, the pitch curve equation of the driven gear, which is conjugate to the driving non-circular gear, can be expressed as:

$$\begin{cases} r_2(\varphi_1) = a - r_1(\varphi_1), \\ \varphi_2 = \displaystyle\int_0^{\varphi_1} \frac{1}{i_{12}(\varphi_1)}\,\mathrm{d}\varphi_1. \end{cases} \tag{3.2}$$

3.1. Mathematical model of pitch curve in the working period

It can be observed from Fig. 4 that the slider velocities at $\varphi_1 = \theta_1$ and $\varphi_1 = \theta_2$ are v_1 and v_2, respectively, and the velocity curve satisfies the following constraint equations in the first motion segments:

$$\begin{cases} v_b(0) = 0, \\ v_b(\theta_1) = v_1, \\ v_b(\theta_2) = v_2. \end{cases} \tag{3.3}$$

The acceleration curve satisfies the following constraint equations in the first motion segments:

$$\begin{cases} a_b(\theta_1) = 0, \\ a_b(\theta_2) = 0. \end{cases} \tag{3.4}$$

In the second motion segments, the velocity and displacement curves should satisfy the following conditions:

$$\begin{cases} v_c(\theta_2) = v_2, \\ s_c(\theta_2) = s_b(\theta_2). \end{cases} \tag{3.5}$$

If the acceleration at the beginning of return stroke is a_1 for the third motion segments, then the following conditions will hold:

$$\begin{cases} a_d(\theta_3) = 0, \\ a_d(\theta_4) = a_1. \end{cases} \tag{3.6}$$

If the slider displacement at $\varphi_1 = \theta_4$ is H, then the velocity and displacement curves in the third motion segments also meet the following conditions:

$$\begin{cases} v_d(\theta_3) = v_2, \\ v_d(\theta_4) = 0, \\ s_d(\theta_4) = H, \\ s_d(\theta_3) = s_c(\theta_3). \end{cases} \tag{3.7}$$

The polynomial coefficients can be determined using Eqs. (3.3)–(3.7) when the center distance a, the crank length $(O_2A)l_2$ and the connecting rod length $(AC)l_3$, the maximum velocity v_1 in the working period, the velocity v_2 in constant speed period, the acceleration a_1 at the beginning of the return period, the maximum slider displacement H and the values of angle θ_1, θ_2, θ_3, θ_4 are given.

By substituting the polynomial coefficients b_0, b_1, b_2, b_3, b_4, b_5 into Eqs. (2.4) and (2.5), c_0 and c_1 into Eqs. (2.7) and (2.8), and d_0, d_1, d_2, d_3, d_4 into Eqs. (2.10) and (2.11), the pitch curve equations in the first, second and third movement periods can be determined for non-circular gears by using Eqs. (2.3), (3.1) and (3.2), respectively. Similarly, by changing the given values of the above parameters, the pitch curve shape of non-circular gears and the rotation range of each movement period can also be changed.

3.2. Mathematical model of pitch curve in the return period

In a rotation cycle, when the transmission ratio function in part of the rotation interval is known, the transmission ratio in the other rotation interval can be established using the compensation method, according to the closed condition of the pitch curve [23]. As shown in Fig. 5, the transmission ratios of the working section and the return section are represented as i_{12} and $i_{12\mathrm{h}}$, respectively. The transmission ratio of the working period has been obtained in Subsec. 3.1. Using the compensation method, the transmission ratio of the return period can be obtained. To simplify the integration and derivation process, it is assumed that the transmission ratio function of the return period can be expressed as the following polynomial:

$$i_{12\mathrm{h}} = e + f_0\varphi_1 + f_1\varphi_1^2 + f_2\varphi_1^3 + f_3\varphi_1^4 + f_4\varphi_1^5, \tag{3.8}$$

where parameter e is a constant and f_0, f_1, f_2, f_3, f_4, and f_5 are polynomial coefficients. It is common for e to be obtained through trial and error. When the obtained transmission ratio function cannot meet the pressure angle or the root-cut condition of the pitch curve, it can be changed by adjusting the coefficient e.

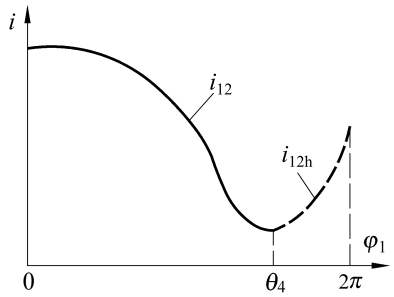

FIG. 5. Schematic diagram of the transmission ratio function in one cycle.

According to the closed requirements of the pitch curve, the transmission ratio function curves of the working and return periods should meet the numerical conditions and smooth connection conditions, expressed in Eq. (3.9):

$$\begin{cases} i_{12}(\theta_4) = i_{12\mathrm{h}}(\theta_4), \\ i_{12}(0) = i_{12\mathrm{h}}(2\pi), \\ i'_{12}(\theta_4) = i'_{12\mathrm{h}}(\theta_4), \\ i'_{12}(0) = i'_{12\mathrm{h}}(2\pi). \end{cases} \tag{3.9}$$

Since the numbers of rotation cycles of the driving gear and driven gear are the same, the corresponding rotation angle of the driven gear when it completes one cycle should be 2π, as seen in Eq. (3.10):

$$\varphi_{2\mathrm{g}} + \varphi_{2\mathrm{h}} = 2\pi, \tag{3.10}$$

where angle $\varphi_{2\mathrm{h}}$ is the rotation angle of the return period of the driven gear, and angle $\varphi_{2\mathrm{g}}$ is the rotation angle of the driven gear during the working period. The total rotation angle of the driven gear during the first, second, and third motion segments is equivalent to the rotation angle of the working period of the driven gear. This can be expressed as:

$$\varphi_{2\mathrm{g}} = \int_0^{\theta_2} \frac{1}{i_{12}}\,\mathrm{d}\varphi_1 + \int_{\theta_2}^{\theta_3} \frac{1}{i_{12}}\,\mathrm{d}\varphi_1 + \int_{\theta_3}^{\theta_4} \frac{1}{i_{12}}\,\mathrm{d}\varphi_1, \tag{3.11}$$

$$\varphi_{2\mathrm{h}} = \int_{\theta_4}^{2\pi} \frac{1}{i_{12\mathrm{h}}}\,\mathrm{d}\varphi_1. \tag{3.12}$$

The values of polynomial coefficients f_0, f_1, f_2, f_3, f_4, and f_5 can be obtained from Eqs. (3.9)–(3.12). By substituting these values into Eqs. (3.8), along with Eqs. (3.1) and (3.2), the pitch curve equation of non-circular gear in the return period can be obtained.

After completing the design of the working and return periods of the non-circular gear, the gear must be divided according to the closed non-circular gear's design requirements so that the length of the pitch curve can be integrated into the entire tooth profile. The commonly used tooth division method involves adjusting the center distance, modulus and number of teeth, or changing the position [24]. In order to avoid repeating the design process, this paper uses the method of adjusting the center distance.

4. Design examples

4.1. Pitch curve model of non-circular gear

For comparison, the parameters of the slider-crank mechanism of Johndel 349 square baler are examined. The basic preset parameters are shown in Table 1. According to the design principles outlined in Sec. 2, the pitch curve of the non-circular gear can be established using MATLAB software. The pitch curves of the driving and driven non-circular gears are shown in Fig. 6 and Fig. 7, respectively. The solid line represents the working period, and the dashed line

Table 1. Initial parameters.

Parameter	Unit	Value
Angle θ_1	rad	$2\pi/5$
Angle θ_2	rad	$7\pi/10$
Angle θ_3	rad	π
Angle θ_4	rad	$13\pi/10$
$O2A$ crank length l_2	mm	380
AC connecting rod length l_3	mm	960
Center distance a	mm	200
Max. speed of working period v_1	mm/s	1600
Constant speed movement v_2	mm/s	1100
Acceleration at the beginning of return period a_1	mm/s^2	-1500
Max. slider displacement H	mm	760
Tooth numbers	–	25
Modulus	mm	3
Constant e	–	0

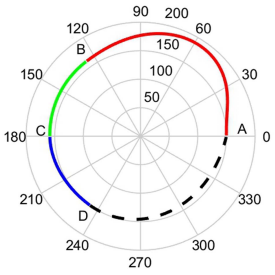

FIG. 6. Pitch curve for the driving non-circular gear.

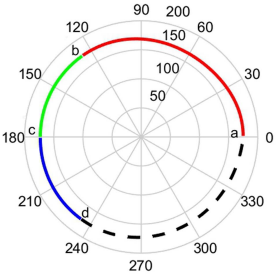

FIG. 7. Pitch curve for the driven non-circular gear.

represents the return period. The AB, BC, and CD segments in the driving gear engage with the ab, bc, and cd segments in the driven gear, respectively. When

the AB segment of the driving gear engages with the ab segment of the driven gear, the slider experiences acceleration followed by deceleration. During the engagement of the BC and the bc segments, the slider achieves a constant speed and when the CD and the cd segments engage, the slider decelerates. When the DA segment of driving gear engages with the da segment of the driven gear, the slider enters the return stage. One cycle of the driving gear is equal to one cycle of the driven gear. Using the involute as the tooth profile curve of the non-circular gear, a three-dimensional model of the non-circular gear can be established by using the conversion tooth profile method, resulting in a complete assembly of the non-circular gear is assembled. After verification, it is confirmed that there is no meshing interference, and the assembly diagram is shown in Fig. 8.

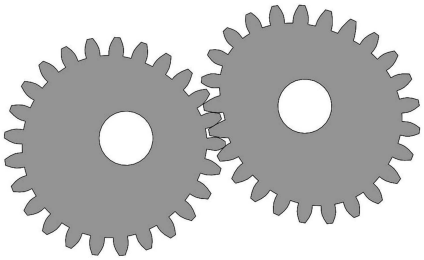

FIG. 8. Assembly diagram of the non-circular gear.

It was observed from establishing the pitch curve that:

1) The pitch curve's shape for the non-circular gear is influenced by the predefined slider movement characteristic curve. By changing the shape of the displacement, velocity and acceleration curves of the slider, the pitch curve of the non-circular gear can be controlled effectively.
2) Before establishing the gear-crank slider mechanism, the maximum velocity v_1 during the slider's working period, as well as the velocity v_2 during the constant speed movement period should be identified. Additionally, the acceleration a_1 and the maximum displacement h of the slider at the beginning of the return period should also be identified beforehand. This allows the non-circular gear to be inversely designed according to the slider's movement performance, improving the non-circular gear-crank slider mechanism's movement performance.
3) By changing the values of angles θ_1, θ_2, θ_3, and θ_4 for the driving gear, the corresponding gear rotation angle for both the working and return periods can be controlled. This flexibility, based on other practical requirements, enables the design of non-circular gear pitch curves that adhere to various practical movement laws.

4.2. Movement characteristics of the non-circular gear-crank slider hay baler mechanism

The ADAMS software is used for simulation to verify the slider movement characteristics and ensure the velocity and acceleration curves align with the preset shapes. In the simulation setup, the input shaft gear and output shaft gear are configured as rotational pairs with the ground, both positioned on the same plane and separated by the theoretical center distance. Additionally, two connecting rod and sliders were incorporated into the model

The following parameters were used in the simulation: elastic modulus E of the two gears: 201 GPa, Poisson's ratio μ: 0.29, damping value: 100 Ns/mm, collision index value of 2.2, and the collision depth value of 0.1 mm. The Coulomb friction model is used for friction between the contact bodies, and the dynamic and static frictions are considered. When lubrication occurs, the dynamic and static friction coefficients were set to 0.05 and 0.08, respectively. A drive was applied to the input shaft in order to simulate the changes in speed and acceleration of the slider within the non-circular gear group during each cycle. The rotational speed was set to 20 r/min to maintain a slow input shaft speed. The slider displacement curve obtained by the simulation is shown in Fig. 9, while the corresponding slider velocity and acceleration curves are shown in Fig. 10.

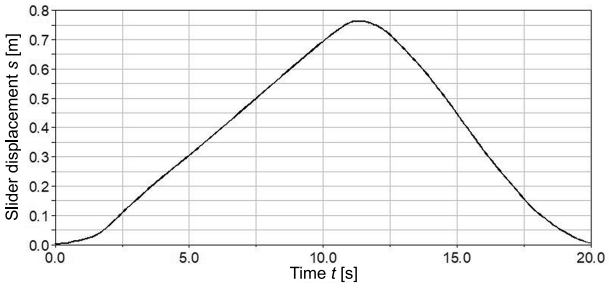

FIG. 9. Slider displacement curve obtained from the simulation.

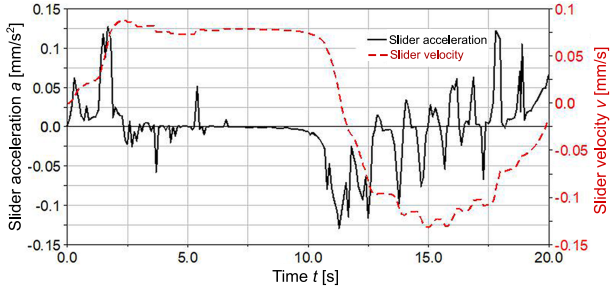

FIG. 10. Velocity and acceleration curves of the slider obtained from the simulation.

The simulation results show that:

1) One cycle of the driving non-circular gear corresponds to one cycle of the driven non-circular gear. The working movement period, which includes the first, second and third motion segments, as well as the return movement period of the slider match the driving and driven non-circular gear movement periods, respectively.
2) The displacement curves in Fig. 9 and Fig. 4 both show a trend of initially increasing and then decreasing, resulting in a parabolic shape.
3) In Fig. 10, the velocity of the slider rapidly increases, then decreases to a suitable speed for compression, and finally quickly returns to its original position. This behavior is consistent with the preset shape in Fig. 4, thereby validating the proposed design.
4) Before compression, the acceleration in Fig. 10 changes from a positive value to a negative value, and then reaches zero to begin constant velocity compression. After compression, the acceleration changes from a negative value to a positive value, and eventually returns to zero. In this context, the shape of the acceleration curve in Fig. 10 generally aligns with the preset shape in Fig. 4. However, there are some numerical differences between the two curves, particularly in the latter half of the curve. The discrepancies in curves may be attributed to impacts and vibrations caused by gaps between motion pairs or variations in motion parameters.

4.3. Characteristics comparison of the new hay baler mechanism and other mechanisms

4.3.1. Comparison of displacement, velocity and baling time. According to existing literature [4], the calculated maximum speed of the non-circular gear-crank slider mechanism in the compression stage is 2100 mm/s, and the calculated compression speed is 820 mm/s. The proposed baler mechanism, as detailed in Table 1 (see parameters v_1 and v_2 in Table 1), aligns with these initial requirements. The results validated in Subsec. 4.1 and 4.2 demonstrate that the proposed baler mechanism, which incorporates acceleration in its design, can achieve constant low-speed compression during the high-pressure stage. Additionally, it allows for pre-control of both the maximum speed and compression speed throughout the compression stage. This innovative baler mechanism approach improves work stability and compression quality compared to existing mechanisms.

To further analyze the variations, the displacement curve of the baler mechanism is plotted in Fig. 11 by substituting the obtained polynomial coefficients into Eqs. (2.4), (2.7), and (2.10). Similarly, the velocity curve is presented in Fig. 1, derived 2 by substituting the polynomial coefficients into Eqs. (2.5),

(2.8), and (2.11). A comparative study of these curves with those of the baler mechanism described in [4] has been carried out.

According to Figs. 11 and 12, the following conclusions can be drawn:

(i) The shapes of the two displacement curves are not significantly different for both mechanisms, and their maximum displacements are both 760 mm.

(ii) The maximum speed and compression speed of the slider in the proposed baler mechanism are 1600 mm/s and 1100 mm/s, respectively. In comparison, the maximum speed and the compression speed of the slider in [4] are 2100 mm/s and 820 mm/s, respectively. This indicates that the proposed mechanism achieves a lower maximum speed and a higher compression in the proposed mechanisms than that of the slider in [4]. In other words, there is less speed fluctuation, which is beneficial for reducing vibration and impact, thereby improving working stability.

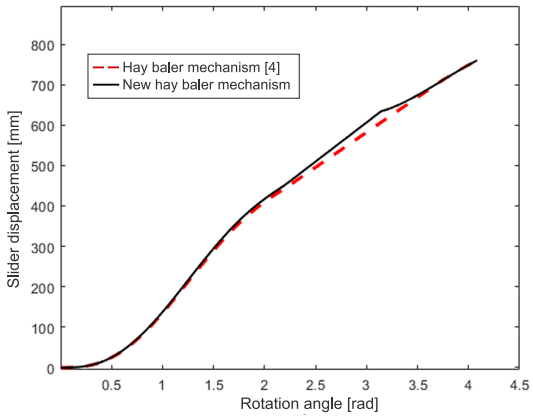

FIG. 11. Displacement comparison chart.

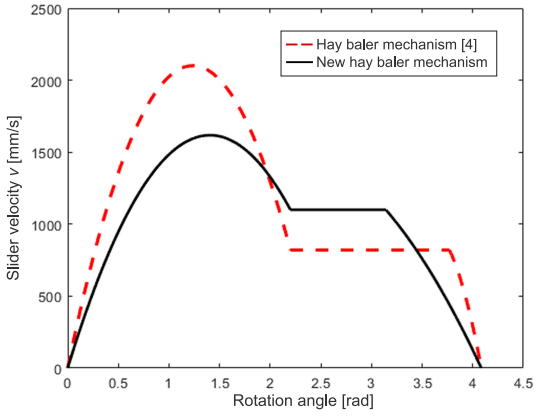

FIG. 12. Velocity comparison chart.

In the existing literature, the crank rotates a total of 234° during the compression process of the non-circular gear-crank slider mechanism [4]. In contrast, in a traditional John Deere 349 square baler, the crank rotates a total of 180° during its compression process. In terms of compression time, the baling time for the proposed mechanism is 30% longer than that of the traditional baler [4]. The crank rotation angle, denoted as θ_4 in Table 1, can be preset according to specific requirements for the proposed baler mechanism. To align with the crank rotation angle of 234° during the compression process described in the existing literature [4], the value of θ_4 is set to $13\pi/10$.

4.3.2. Power comparison. The power required for the hay baler mechanism can be calculated during the compression stage by using the following formula:

$$P = Fv, \tag{4.1}$$

where, speed v is the slider moving speed, and resistance F is the slider resistance during the compression process. The relationship between F and slider displacement can be expressed as [15]:

$$F = 2.498\times10^{-7}s^4 - 1.575\times10^{-4}s^3 + 1.846\times10^{-2}s^2 + 3.447s - 131.2779. \tag{4.2}$$

By substituting the obtained polynomial coefficients into the speed curves in Eqs. (2.5), (2.8), and (2.11), the power curve of the proposed baler mechanism can be drawn according to Eq. (4.1). The power curve of the baler mechanism presented in [4] is also shown for comparison in Fig. 13. It can be seen from Fig. 13 that the maximum power of the proposed baler mechanism is 6300 W, while the maximum power in [4] is 18 750 W. Therefore, without compromising productivity, the proposed baler mechanism can significantly reduce the required baling power. There is a 66.4% reduction in the required maximum power. This reduction allows for the use of a relatively small motor in the new baler, effectively addressing the issue of power imbalance in hay balers [25].

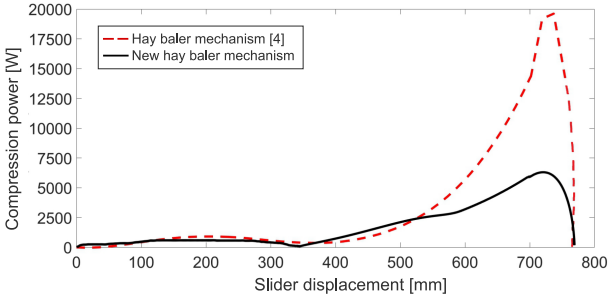

FIG. 13. Power comparison chart.

4.3.3. Acceleration comparison. As illustrated in Fig. 14, by substituting the obtained polynomial coefficients into the acceleration curves in Eqs. (2.6), (2.9), and (2.12), the slider acceleration curve in the proposed baler mechanism can be drawn. The slider acceleration curve from [4] is also shown for comparison in Fig. 14. The slider acceleration curve from [4] corresponds to the left vertical axis, with a maximum acceleration of $45\,000\ \mathrm{mm}\cdot\mathrm{s}^{-2}$. In contrast, the slider acceleration curve for the proposed mechanism is represented on the right vertical axis, showing a maximum acceleration of only $1500\ \mathrm{mm}\cdot\mathrm{s}^{-2}$, which is an order of magnitude difference between the two mechanisms. Therefore, the application of the new hay baler mechanism is beneficial to reduce the inertial force generated by high-speed slider movement, thus reducing vibration during operation.

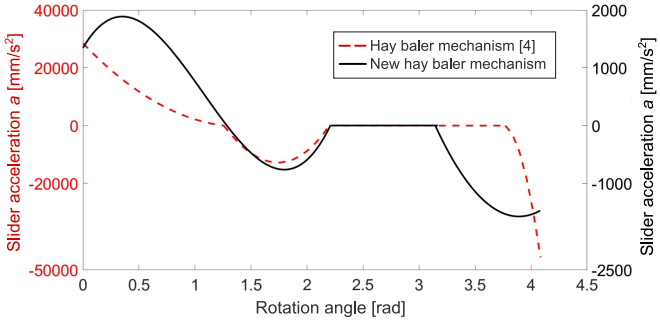

FIG. 14. Acceleration comparison chart.

5. CONCLUSIONS

This paper presents an ideal kinematic curve for the slider and the description method of its polynomial function for the non-circular gear-crank slider hay baler mechanism. The mathematical models of the non-circular gear pitch curves in both the working and return periods of the slider were established. The design method has been verified by numerical simulation, and the main conclusions can be drawn as follows:

1) By changing the parameters of the established movement characteristic curve, such as the center distance a, crank O_2A length l_2, connecting rod AC length l_3, maximum velocity v_1 during the working period, velocity v_2 during the constant speed movement period, acceleration a_1 at the beginning of return, maximum slider displacement H, etc., the shape of the pitch curve of the non-circular gear can be controlled. Additionally, the non-circular gear pitch curve with other movements of the slider can be designed according to requirements.

2) Before establishing the non-circular gear-crank slider mechanism, the acceleration and velocity of the slider should be identified to reduce vibrations and impact of the non-circular gear-crank slider mechanism.
3) By changing the values of the driving gear rotation angles θ_1, θ_2, θ_3, and θ_4, the rotation angle of the gears corresponding to the working and return periods can be manipulated to adjust the baling time. Theoretically, the baling time of new hay baler mechanism can be designed to be arbitrary small.
4) Speed fluctuations have been reduced, and the slider acceleration and baling power of the proposed baler mechanism have also been significantly decreased. Compared with the existing non-circular gear-crank slider hay baler mechanism, the maximum power required by the proposed baler mechanism can be reduced by about 66.4%, and its maximum acceleration is reduced by an order of magnitude.

Acknowledgments

This work was supported by the National Natural Science Foundation of China under Grants No. 51205335 and No. 52205055, and the Scientific Research for the High-Level Talent at Nanjing Institute of Technology under Grant No. YKJ201702. These financial supports are gratefully acknowledged. The authors also sincerely appreciate the comments and suggestion for modification made by the editors and anonymous referees.

References

1. Li D.B., *The parameter optimization and virtual experiment and test of hay baler compression mechanism* [in Chinese], Doctoral Thesis, Zhejiang: Zhejiang Sci-Tech University, 2011.

2. Zhou G.D., Du J.M., She W.L., Zhao D.Y., Hao F., Experimental study on stress relaxation of forage in compression process and mechanics research of compression piston [in Chinese], *Journal of Agricultural Mechanization Research*, **39**(4): 197–201, 2017.

3. Bortolini M., Cascini A., Gamberi M., Mora C., Regattieri A., Sustainable design and life cycle assessment of an innovative multi-functional haymaking agricultural machinery, *Journal of Cleaner Production*, **82**(3): 23–36, 2014, doi: 10.1016/j.jclepro.2014.06.054.

4. Lei C.Y., Chen J.N., Li P.P., Wang Y., Reverse design of non-circular gear-crank slider hay baler mechanism [in Chinese], *Transactions of the Chinese Society of Agricultural Engineering*, **28**(13): 22–27, 2012.

5. Teffera A., Tekeste S., Denekew Y., On-farm evaluation and demonstration of different types of hay press, *Livestock Research for Rural Development*, **24**(1): 11–13, 2012, http://www.lrrd.org/lrrd24/1/teff24001.htm.

6. Coblentz W.K., Fritz J.O., Bolsen K.K., Baling system for making laboratory-scale hay bales, *Agronomy Journal*, **85**(4): 962–965, 1993, doi: 10.2134/agronj1993.00021962008500040032x.

7. Wang C.G., Tan L.D., Study on a virtual prototype based hay highly compressing process [in Chinese], *Transactions of the Chinese Society for Agricultural Machinery*, **36**(3): 99–101, 2005.

8. Zhao H.G., *Simulation research on dynamic characteristic of hay baler* [in Chinese], Doctoral Thesis, Harbin: Northeast Forestry University, 2007.

9. Li D.B., Jiang P.P., Luo H., Zhao Y., The optimization and simulation of the six-shaft hay baler's parameters [in Chinese], *Journal of Zhejiang Sci-Tech University*, **29**(3): 208–213, 2012.

10. Chen P.Y., Wu P., Ma Y.H., Wang H.Y., Xue D.M., Design of cam-type hay balers based on hay compression characteristics [in Chinese], *Journal of Agricultural Mechanization Research*, **41**(8): 88–93, 102, 2019.

11. Dawei L., Tingzhi R., Study on deformed limacon gear and motion optimization of its serial mechanism, *Journal of Mechanical Design, Transaction of ASME*, **133**(6): 061004-1–8, 2011, doi: 10.1115/1.4004116.

12. Medvecká-Beňová S., Designing pitch curves of non-circular gears, *Scientific Journal of Silesian University of Technology. Series Transport (Zeszyty Naukowe Politechniki Śląskiej. Seria Transport)*, **99**: 105–114, 2018, doi: 10.20858/sjsutst.2018.99.10.

13. Vasie M., Andrei L., Design and generation of noncircular gears with convex-concave pitch curves, *Annals of "Dunarea de Jos" University of Galati*, *Fascicle V*, *Technologies in Machine Building*, **30**(2): 55–60, 2012, https://www.gup.ugal.ro/ugaljournals/index.php/tmb/article/view/1728.

14. Ottaviano E., Mundo D., Danieli G.A., Ceccarelli M., Numerical and experimental analysis of non-circular gears and cam-follower systems as function generators, *Mechanism and Machine Theory*, **43**(8): 996–1008, 2008, doi: 10.1016/j.mechmachtheory.2007.07.004.

15. Guo C.Z., Fu W., Zhu J.C., Zhao C.G., Design of the pitch curves of non-circular gear for quick return mechanism [in Chinese], *Chinese Journal of Mechanical Engineering*, **141**(11): 221–227, 2005.

16. Niu S.C., Li G., Li G.Y., Huyang J.J., The design of new transmission in automatic fixation-shaping machine [in Chinese], *Journal of Agricultural Mechanization Research*, **33**(2): 58–61, 2011.

17. Hu Z.Y., Yang H., Li D.Z., Han J., Optimization design and experimental analysis of non-circular gears for constant flow pumps [in Chinese], *China Mechanical Engineering*, **27**(22): 3082–3087, 2016.

18. Chen X.B., Iwatsuki N., Hayashi I., Morikawa K., Synthesis of function generators composed of non-circular gear-linkage based on L'Hospital's theorem [in Chinese], *Journal of Tongji University*, **20**(9): 1091–1094, 2002.

19. Langer T.H., Ebbesen M.K., Kordestani A., Experimental analysis of occupational whole-body vibration exposure of agricultural tractor with large square baler, *International Journal of Industrial Ergonomics*, **47**(2): 79–83, 2015, doi: 10.1016/j.ergon.2015.02.009.

20. Song D., Wang G., Xue Z., Zhang J., Huang Z., Yang Z., Design and analysis on compression mechanism of small square bales of sugarcane leaf Baler, *Agricultural Science & Technology*, **15**(10): 1812–1815, 2014.

21. Yang M.S., Li X.Y., An analysis of open compression procedure of herbage material [in Chinese], *Journal of Agricultural Mechanization Research*, **27**(3): 81–86, 2005.

22. Litvin F.L., Gonzalez-Perez I., Fuentes A., Hayasaka K., Design and investigation of gear drives with non-circular gears applied for speed variation and generation of functions, *Computer Methods in Applied Mechanics & Engineering*, **197**(45–48): 3783–3802, 2008, doi: 10.1016/j.cma.2008.03.001.

23. Liu D.W., Ren T.Z., Creating pitch curve of closed non-circular gear by compensation method [in Chinese], *Chinese Journal of Mechanical Engineering*, **47**(13): 147–152, 2011.

24. Litvin F.L., Fuentes A., *Gear Geometry and Applied Theory*, 2nd ed., Cambridge University Press, 2004.

25. Yang M.S., Wang C.G., The analysis on essential problems in hay compressing engineering [in Chinese], *Transactions of the Chinese Society of Agricultural Engineering* (*Transactions of the CSAE*), **13**(5): 134–138, 1997.

Received April 10, 2024; accepted version September 26, 2024.
Online first October 14, 2024.